Electronic Supplementary Material (ESI) for Dalton Transactions.
This journal is © The Royal Society of Chemistry 2021

Supporting Information

Electrocatalytic Syngas Generation with a Redox Non-Innocent Cobalt 2-Phosphinobenzenethiolate Complex

Nicholas M. Orchanian, Lorena E. Hong[†]*, David A. Velazquez*[†]*, Smaranda C. Marinescu**

[†] equal contribution

Department of Chemistry, University of Southern California, Los Angeles, California 90089, United States

Corresponding Author

*smarines@usc.edu

Experimental Methods

Materials and Synthesis

All manipulations of air- and moisture-sensitive materials were conducted under nitrogen atmosphere in a Vacuum Atmospheres glovebox or on a dual manifold Schlenk line with oven-dried glassware. Water was deionized with the Millipore Synergy system (18.2 MΩ·cm). All other solvents used were degassed with nitrogen, passed through activated alumina columns, and stored over 4Å Linde-type molecular sieves. Proton NMR spectra were acquired using a Varian 400-MR 2-Channel spectrometer at room temperature and referenced to the residual ^{1}H resonances of the deuterated solvent (^{1}H: benzene-d_6, δ 7.16 ppm). The desired ligand was synthesized according to the reported literature procedure.[1] CoPS was synthesized using an analogous procedure to those reported for similar complexes.[1] All other chemical reagents were purchased from commercial vendors and used without further purification. Elemental analyses were performed by Robertson Microlit Laboratories, Ledgewood, New Jersey.

Synthesis of $Co(PiPr_2SC_6H_4)_2$ (CoPS)

The desired 2-(diisopropylphosphaneyl)benzenethiol ligand was prepared according to the literature procedure.[1] In an inert-atmosphere glovebox, a Schlenk flask was charged with *n*-BuLi (15.8 mL), tetramethylethylenediamine (5.9 mL), and cyclohexane (12.0 mL). This reaction mixture was transferred to a Schlenk line and cooled to 0 °C. A separate flask was charged with thiophenol (1.9 mL) and cyclohexane (4.8 mL), sparged with N_2, then cooled to 0 °C. The thiophenol solution was transferred dropwise via cannula to the Schlenk flask charged with *n*-BuLi, and the reaction mixture was maintained at 0 °C for 30 min. The reaction mixture

was then allowed to warm to room temperature with stirring over-night. After overnight reaction the dilithiated product, $Li_2SC_6H_4$, was obtained as a white suspension, which was subsequently isolated by air-free filtration. The resulting solid was washed with three portions of 10 mL pentane before drying under reduced pressure for one hour to afford a white solid. The white solid was dissolved in THF (20.0 mL), yielding a red-orange solution. A separate flask was charged with *i*Pr_2PCl (2.0 mL) and THF (2.0 mL), and both flasks were cooled to -78 °C. Once cooled, the phosphine solution was transferred dropwise via cannula to the red-orange solution of $Li_2SC_6H_4$. The reaction mixture was maintained at -78 °C for 30 min., before it was allowed to warm to room temperature with stirring overnight. Following overnight stirring, a yellow solution was observed, which was acidified with a N_2-sparged solution of HCl (1.5 mL) in DI water (18.0 mL) at 0 °C. The organic layer of the resulting biphasic solution was transferred to a clean flask via cannula and the aqueous layer was extracted with three portions of 5 mL diethyl ether. The combined organic phases were dried with $MgSO_4$ and collected by air-free filtration. The resulting yellow-brown solution was reduced to a brown oil under vacuum and purified by vacuum distillation. The distilled product was diluted with methanol (8 mL) and treated with triethylamine (0.7 mL). Excess anhydrous cobalt(II) chloride (580 mg) was added in one portion to the pale-yellow ligand solution, causing an immediate color change to vivid yellow. This solution was allowed to stir overnight. The crude **CoPS** product was collected by filtration and dried under reduced pressure. Crystals suitable for crystallographic and electrochemical characterization were prepared by recrystallization in air through layering of methanol over a concentrated solution of **CoPS** in benzene at 6 °C (80% yield). ^{1}H NMR (400 MHz, benzene-d_6) δ 24.9 (s, 2H, Ph*H*), 11.2 (s, 2H, Ph*H*), 4.8 (br s, 12H, -CH(C*H*$_3$)$_2$), 2.5 (br s, 4H, -C*H*(CH$_3$)$_2$), -

0.5 (br s, 12H, -CH(C*H*$_3$)$_2$), -16.1 (s, 2H, Ph*H*), -22.5 (s, 2H, Ph*H*). Anal. Calcd. ($C_{24}H_{36}CoP_2S_2$): C, 56.57; H, 7.12; Co, 11.56; Found: C, 56.38; H, 6.89; Co, 10.88.

Synthesis of Reduced CoPS Complex

In a nitrogen-filled glovebox, a 20 mL vial was equipped with a glass stir bar, and charged with 0.1311 g (0.258 mmol) of CoPS. Approximately 5 mL of tetrahydrofuran (THF) was added to the vial, and the reaction mixture was allowed to stir until the solution was a homogeneous transparent dark orange color. Approximately 0.349 g (2.58 mmol) of KC_8 was added in excess to the reaction mixture, and the solution turned into a black opaque color with a green hue after 1 h of mixing. The reaction mixture was then filtered to remove oxidized KC_8, and the green filtrate was collected in a separate vial. Diffusion of pentane into the mother liquor generated dark greenish red crystals (28% yield). ^{1}H NMR (500 MHz, benzene-d_6) δ 7.49 (s, 2H, Ph*H*), 7.34 (s, 2H, Ph*H*), 6.90 (s, 2H, Ph*H*), 6.55 (s, 2H, Ph*H*), 1.98 (br s, 4H, -C*H*(CH$_3$)$_2$), 1.11 (br s, 24H, -CH(C*H*$_3$)$_2$). Anal. calcd. ($C_{24}H_{36}CoKP_2S_2$): C, 49.05; H, 6.17; Found: C, 45.55; H, 6.28.

X-Ray Crystallography

CoPS: A clear orange prism-like specimen was mounted for the X-ray crystallographic analysis, with approximate dimensions of 0.198 mm × 0.214 mm × 0.368 mm. The X-ray intensity data were measured on a Bruker APEX DUO system equipped with a fine-focus tube (MoKα, λ = 0.71073 Å) and a TRIUMPH curved-crystal monochromator, with a theta range of 1.96 to 30.47°. A total of 2520 frames were collected during a 7-hour exposure time.

[CoPS]$^-$: A red prism-like specimen was mounted for analysis, with approximate dimensions of 0.050 mm × 0.079 mm × 0.470 mm. The X-ray intensity data were measured on a

Bruker APEX DUO system equipped with a fine-focus tube (MoKα, λ = 0.71073 Å) and a TRIUMPH curved-crystal monochromator, with a theta range of 1.96 to 30.47°. A total of 2520 frames were collected during a 21-hour exposure time.

For both samples, the frames were integrated with the Bruker SAINT software package using a SAINT V8.38A (Bruker AXS, 2013) algorithm. Data were corrected for absorption effects using the multi-scan method (SADABS). The SHELXTL XT 2014/5 (Bruker AXS, 2014) Software Package was used to determine the structure solution with direct methods.[2] The SHELXTL XT 2014/5 (Bruker AXS, 2014) Software Package was used for refinement by full-matric least-squares on F2.[2] Additional details are provided in **Tables S1–S8**.

Structural parameters were calculated for the coordination complexes studied here, by using the **Equation 1** from Houser and et al, where α is the shortest, and β is the longest bond angle.[14]

$$\tau = \frac{360-(\alpha+\beta)}{141} \qquad \textbf{Eq. 1}$$

Electrochemistry

Electrochemistry experiments were carried out in acetonitrile solution with 0.1 M [nBu$_4$N][PF$_6$] electrolyte using a Pine potentiostat. All cyclic voltammetry and controlled potential electrolysis experiments were carried out with a three electrode configuration in an electrochemical H-cell under a nitrogen or CO_2 atmosphere using glassy carbon working and counter electrodes. The working and counter compartments of the cell were separate by a porous glass frit. Working and counter electrodes were polished using Micropolish powder (purchased from CH Instruments, Inc.) prior to electrochemical studies. Six-sided polished glassy carbon

plate electrodes with working areas of 2.5 cm^2 were used for controlled potential electrolysis studies, and polished glassy carbon disc electrodes with 3 mm diameter (working area = 0.07 cm^2) were used for cyclic voltammetry studies. All current densities presented are normalized to this geometric surface area. The pseudo-reference electrode used was a silver wire purchased from VWR and was isolated from solution with a glass capillary and Vycor frit. All experiments were referenced relative to ferrocene (Fc) with the Fc^+/Fc couple defined as 0 V. Ohmic drop was compensated using positive feedback compensation as implemented in the Aftermath software suite.

NMR

Evans method was applied according to literature precedent.[3] A 1 mM solution of catalyst in benzene-d_6 was prepared and a sealed capillary containing protio-benzene was inserted into the NMR sample tube. The splitting between the solvent peaks was measured by a ^1H NMR spectroscopy study and reported equations were applied to calculate μ_{eff}.[3]

Electrochemical Analysis

Calculation of Faradaic efficiency was performed according to **Equation 2** below, which considers only the total amount of products formed and the total amount of charge passed during the electrolysis experiment. Turnover number (TON) was determined according to **Equation 3** below, which considers the bulk catalyst loading in solution. This provides an underestimate of TON, as only the amount of catalyst within the electrochemical diffusion layer is active during electrolysis studies.

$$FE = \frac{Total\ mols\ of\ product\ formed}{Total\ mols\ of\ electrons\ passed} \qquad \textbf{Eq. 2}$$

$$TON = \frac{Total\ mols\ of\ product\ formed}{Bulk\ catalyst\ loading\ (mols)} \qquad \textbf{Eq. 3}$$

Wash tests were performed by removing the solution of the catalyst from the H-cell *via* syringe under a positive pressure of CO_2, and rinsing the working compartment of the electrolysis cell three times with acetonitrile (**Figure S15**). The cell was maintained under 1 atm of CO_2, and the electrode was not removed from the cell during these washings to prevent O_2-exposure. No visible material is present on the electrode following CPE, and much lower current densities are observed in the wash test relative to any of the preparative CPE studies. As such, these studies strongly suggest that the observed reactivity is due to the solubilized catalyst, as no gaseous products are observed following the three wash cycles.

Gas Chromatography

Gaseous products were quantified using a Shimadzu GC-2010-Plus instrument equipped with a BID detector and a Restek ShinCarbon ST Micropacked column. In a typical experiment, 2 mL of gas were withdrawn from the headspace of the electrochemical cell with a gas-tight syringe and injected into the instrument. Calibration plots were prepared with multiple injections of syngas standards purchased from Praxair, Inc. Faradaic efficiencies were determined by dividing the amount of gaseous product produced as measured by gas chromatography by the amount of gas expected based on the total charge measured during controlled potential electrolysis. Multiple runs were performed for each condition studied, leading to similar behavior. The reported μmol of gas produced (and subsequently FE) are averaged values and error bars are determined from multiple experiments.

Formate Test[13]

Following CPE studies, a 5 mL aliquot of each electrolysis solution was collected and extracted with 2 mL D_2O. The aqueous portion was acidified with one drop of HCl and tested for formate by ^1H NMR spectroscopy. Formate was not detected in any of the experiments

performed. Detection of methanol, aldehydes, and other alcohols was carried out through NMR spectroscopy studies, and detection of methane, carbon monoxide, and hydrogen was carried out through gas chromatography.

Oxalate Test

Controlled potential electrolysis (CPE) was performed at a potential of -2.18 V for 2 h in the presence of 1 mM CoPS under CO_2 atmosphere. A steady current was observed during electrolysis. Post-electrolysis analysis reveals no gaseous products, and the solution of the working electrode compartment in the CPE cell was extracted three times with dichloromethane and pure H_2O. The water layers were combined and an aqueous solution of $CaCl_2$ was added to the reaction mixture. No precipitate was observed in the reaction mixture, but insoluble calcium oxalate was present in the standard of aqueous sodium oxalate.

UV-Vis spectroscopy

UV-Vis spectra were collected using a UV-1800 Shimadzu UV spectrophotometer. Samples were studied in transmittance mode with a 1 cm quartz cuvette, and the spectrum measured for a blank benzene or acetonitrile sample was subtracted as background.

Computational Methods

All calculations were run using the Q-CHEM program package.[5] Geometry optimizations were run with unrestricted DFT calculations at the PBE level of theory with the Pople 6-31G(d) basis set for all atoms.[6,7,8] All optimized geometries were verified as stable minima with frequency calculations at the same level of theory. The PBE functional was used throughout this study, as it provided minimal spin contamination for the reduced complexes. The range-separated hybrid ω-B97xD functional as well as the PBE0 and BP86 functionals were also

tested, but all yielded >20% spin contamination for the singly- and doubly-reduced complexes. Single point energy calculations were run with a larger triple-zeta def2-TZVP basis set for all atoms.[9] Time-dependent density functional theory calculations were run at the B3LYP level of theory with the def2-TZVP basis set for all atoms. Kohn-Sham orbital images are presented with isovalues of 0.05 for clarity. Basis sets were retrieved from the Basis Set Exchange.[10,11]

Table S1. X-ray crystallography data and structure refinement for **CoPS**.

Chemical Formula	**$C_{30}H_{42}CoP_2S_2$**
Formula weight	587.62
Crystal system	Monoclinic
Space group	P 1 21/n 1
a (Å)	11.658(3)
b (Å)	9.739(3)
c (Å)	14.049(4)
α (°)	90
β (°)	111.120(3)
γ (°)	90
V (Å^3)	1487.9(7)
Z	2
D_{calc} (g/cm^3)	1.312
μ (Mo Kα) (mm^{-1})	0.842
F (000)	622
Reflections collected	21559
Independence reflections	4494 [R_{int} = 0.0267]
R_1 $(I > 2\sigma(I))$	0.0208
wR_2 *(all data)*	0.0538
Goodness-of-fit (GOF) on F^2	1.015

Table S2. Selected bond lengths (Å) for **CoPS**.

Co(1)–S(1)	2.1625(4)
Co(1)–P(1)	2.2163(5)
S(1)–C(10)	1.7735(10)
P(1)–C(6)	1.8542(10)
P(1)–C(9)	1.8233(10)
C(9)–C(10)	1.4041(13)

Table S3. Selected bond angles (°) for **CoPS**.

S(1)–Co(1)–S(2)	180.0
P(1)–Co(1)–P(2)	180.0
S(1)–Co(1)–P(1)	90.95(2)
C(10)–S(1)–Co(1)	107.70(4)
C(9)–P(1)–Co(1)	107.49(3)

Table S4. X-ray crystallography data and structure refinement for **KCoPS.**

Chemical Formula	**$C_{24}H_{36}CoKP_2S_2$**
Formula weight	548.62
Crystal system	Monoclinic
Space group	P 1 21/n 1
a (Å)	14.737(5)
b (Å)	8.456(3)
c (Å)	21.227(7)
α (°)	90
β (°)	90.798(5)
γ (°)	90
V ($Å^3$)	2651.2(14)
Z	4
D_{calc} (g/cm^3)	1.375
μ (Mo Kα) (mm^{-1})	0.842
F (000)	1152
Reflections collected	63488
Independence reflections	8126 [R_{int} = 0.0464]
R_1 *(I > 2σ(I))*	0.0333
wR_2 *(all data)*	0.0756
Goodness-of-fit (GOF) on F^2	1.033

Table S5. Selected bond lengths (Å) for **KCoPS**.

Co(1)–S(1)	2.3161(6)
Co(1)–P(1)	2.2203(7)
S(1)–K(1)	3.2037(9)
S(1)–C(1)	1.7768(17)
P(1)–C(2)	1.8277(16)

Table S6. Selected bond angles (°) for **KCoPS**.

S(1)–Co(1)–S(2)	115.93
P(1)–Co(1)–P(2)	149.82
S(1)–Co(1)–P(1)	87.28(2)
C(10)–S(1)–Co(1)	104.43(6)
C(9)–P(1)–Co(1)	122.93(6)

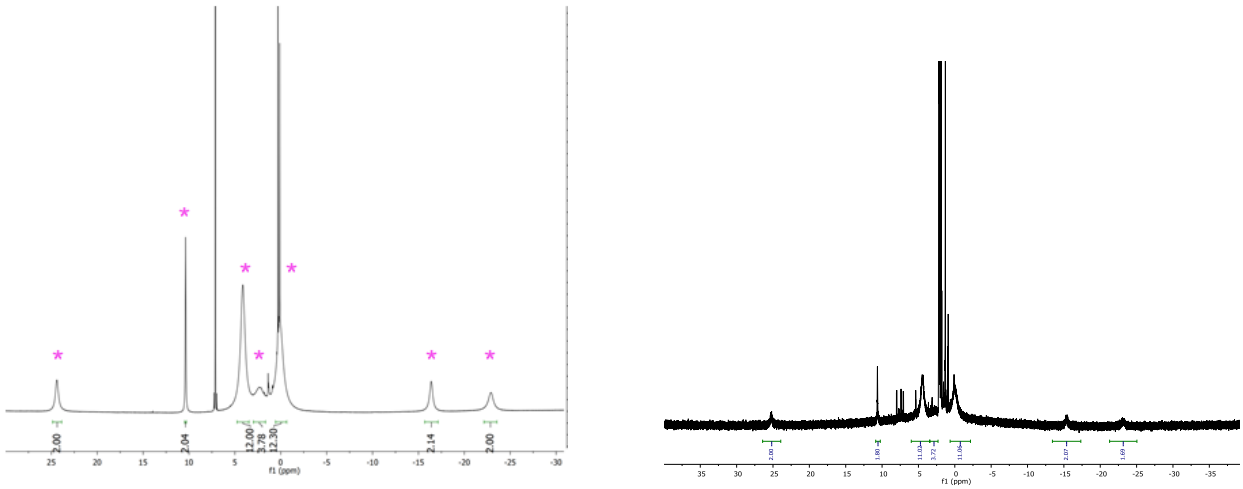

Figure S1. 400 MHz ^{1}H NMR spectrum of 1 mM **CoPS** in a solution of benzene-d_6 (left). Pink asterisks are attributed to the molecular complex. Additional resonances are attributed to the residual solvent. Also shown is a 400 MHz ^{1}H NMR spectrum of 1 mM **CoPS** in a solution of acetonitrile-d_3 (right), exhibiting analogous resonances.

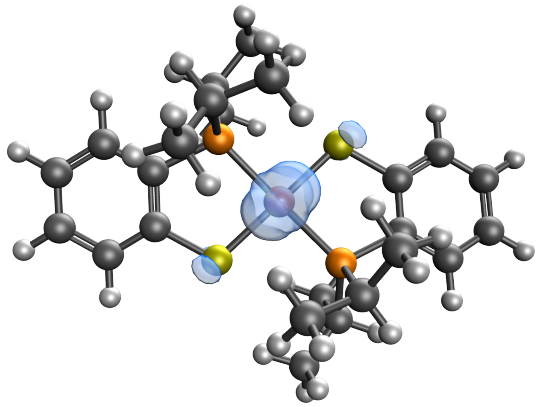

Figure S2. Calculated spin density distribution of **CoPS** at the def2-TZVP/PBE level of theory. Plotted with isovalue = 0.05 for clarity.

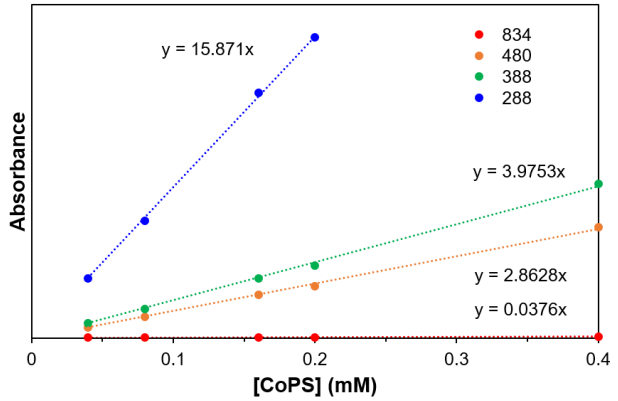

Figure S3. Measured absorbance by UV-Vis spectroscopy for the observed electronic transitions as a function of **CoPS** concentration.

Table S7. Calculation of molar extinction coefficients for **CoPS** measured by UV-Vis spectroscopy based on the dilution studies illustrated in Figure S3..

[CoPS] (mM)	A (834 nm)	A (480 nm)	A (388 nm)	A (358 nm)	A (288 nm)
0.40	0.015	1.164	1.616	1.001	-
0.20	0.007	0.545	0.757	0.488	3.1583
0.16	0.006	0.452	0.628	0.391	2.5787
0.08	0.003	0.219	0.303	0.179	1.2344
0.04	0.001	0.112	0.154	0.086	0.6276
Slope (M^{-1} cm^{-1})	**3.8**	**2862.8**	**3975.3**	**2491.0**	**15871.0**

Table S8. Calculated oscillator strengths and wavelengths of the electronic transitions by TD-DFT and comparison to the experimentally determined transition wavelengths. Only transitions with $f_{calc} \geq 7 \times 10^{-5}$ are shown.

Transition	f_{calc}	λ_{calc} (nm)	λ_{exp} (nm)	|Difference| (nm)
λ_1	7.0×10^{-5}	721	834	113
λ_2	5.9×10^{-4}	482	480	2.0
λ_3	2.7×10^{-3}	416	388	28.8
λ_4	1.8×10^{-2}	394	358	36.6
λ_5	1.2×10^{-2}	390	288	103
			Avg |Difference| (nm)	**56.6**

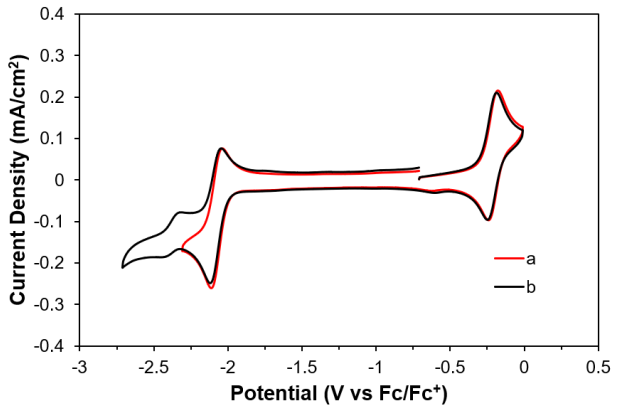

Figure S4. Cyclic voltammetry of **CoPS** (1 mM) in acetonitrile with 0.1 M [nBu$_4$N][PF$_6$] supporting electrolyte (scan rate = 100 mV/s) from 0 V vs Fc/Fc$^+$ to (a) -2.3 V vs Fc/Fc$^+$ and (b) -2.7 V vs Fc/Fc$^+$.

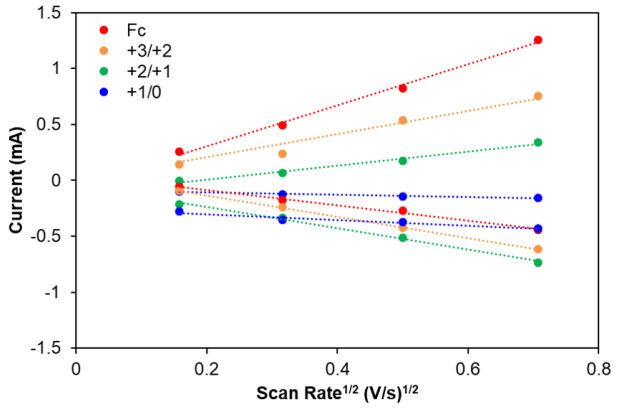

Figure S5. Randles-Sevcik analysis based on variable scan rate experiments. Redox features are labeled by the formal oxidation state of cobalt.

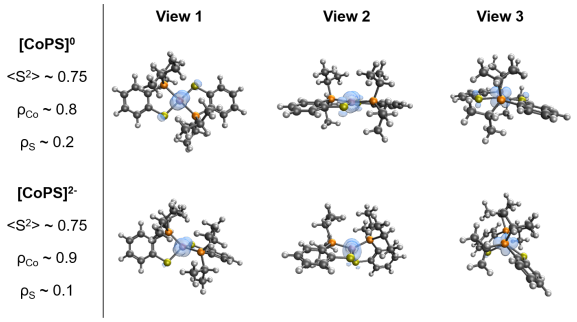

Figure S6. Calculated spin densities for the paramagnetic species, **[CoPS]^0** and **[CoPS]$^{-2}$**, at the def2-TZVP/PBE level of theory. Both species (rows) are depicted in three different views (columns) for clarity.

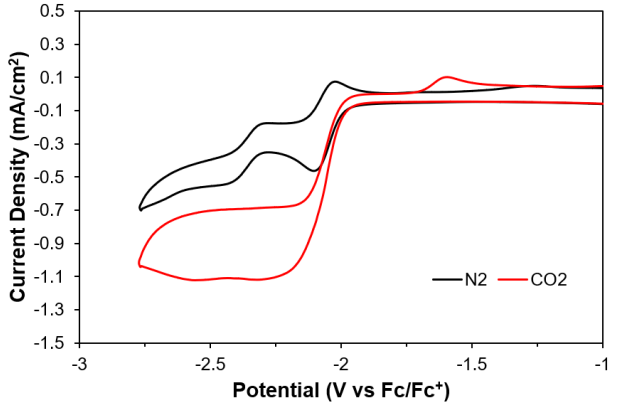

Figure S7. Cyclic voltammograms of 1 mM **CoPS** in an acetonitrile solution with 0.1 M [nBu$_4$N][PF$_6$] electrolyte with scan rate = 100 mV/s under N_2 atmosphere (black) and CO_2 (red).

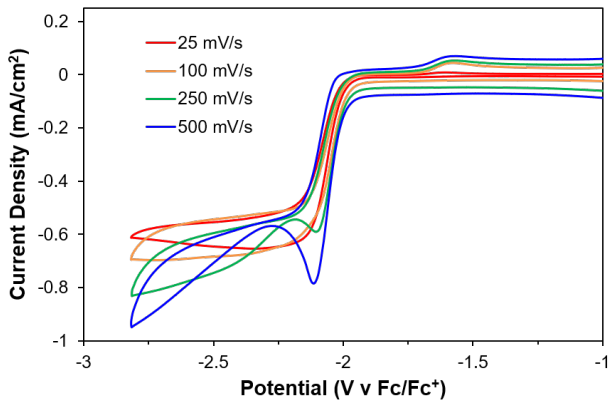

Figure S8. Cyclic voltammetry of 1 mM **CoPS** in acetonitrile under CO_2 atmosphere with 0.1 M [nBu$_4$N][PF$_6$] supporting electrolyte at various scan rates.

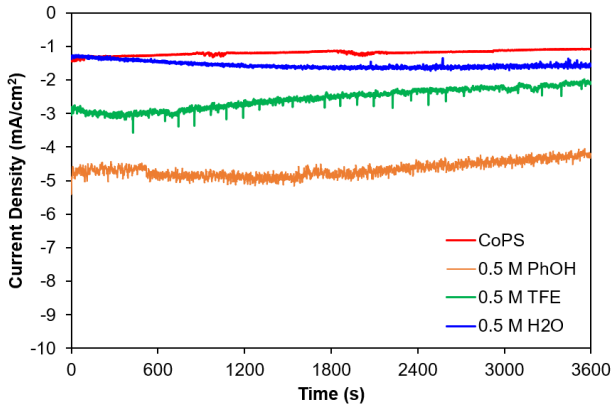

Figure S9. Controlled potential electrolysis traces measured under CO_2 atmosphere. In all cases a solution of 1 mM **CoPS** in acetonitrile (with 0.1 M [nBu$_4$N][PF$_6$] supporting electrolyte) was held at a potential of -2.18 V for 1 hour in the absence of acid (red), presence of 0.5 M PhOH (orange), presence of 0.5 M TFE (green), or presence of 0.5 M water (blue).

Table S9. Summary of CPE results under CO_2. All data presented are averaged quantities of multiple experiments, as reflected in the determined error bars. Charge passed was determined by integration of the CPE trace, and gaseous products were determined by gas chromatography.

	Potential (V)	Duration (h)	Charge (C)	mol H_2	mol CO	TON H_2	TON CO
No acid	-2.18	1	10.23±0.51	-	-	-	-
PhOH	-2.18	1	43.10±2.1	1.83±0.2E-04	4.58±0.4E-05	4.66	1.17
TFE	-2.18	1	25.66±1.3	1.10±0.1E-04	1.05±0.1E-05	2.80	0.27
H_2O	-2.18	1	14.71±0.74	5.48±0.6E-05	2.02±0.2E-05	1.39	0.51
H_2O	-2.18	3	35.88±1.8	1.44±0.1E-04	4.36±0.1E-5	3.66	1.11

Table S10. Summary of FE calculations from CPE experiments under CO_2. All data presented are averaged quantities of multiple experiments, as reflected in the determined error bars. Charge passed was determined by integration of the CPE trace, and gaseous products were determined by gas chromatography.

	Potential (V)	Duration (h)	FE (H_2)	FE (CO)	FE (Total)	H_2/CO
No acid	-2.18	1	-	-	-	-
PhOH	-2.18	1	82±8%	20±2%	>99%	4.1±0.5
TFE	-2.18	1	83±8%	8±1%	91±9%	10.2±1
H_2O	-2.18	1	72±7%	29±3%	99±8%	2.7±0.3
H_2O	-2.18	3	75±7%	23±2%	98±7%	3.3±0.5

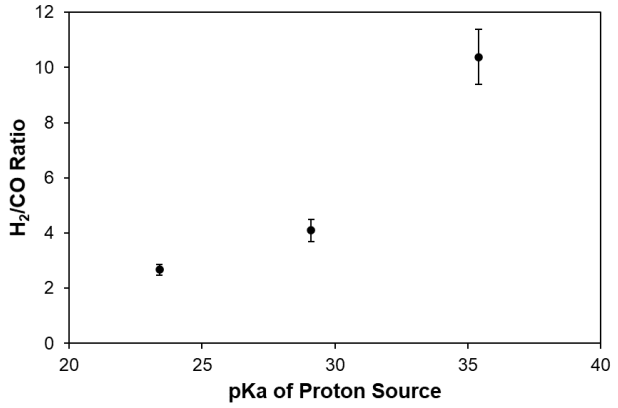

Figure S10. Summary of H_2:CO ratio calculations from CPE experiments. All data presented are averaged quantities of multiple experiments, as reflected in the determined error bars. Gaseous products were determined by gas chromatography. All pK_a estimates based on literature precedent.[12]

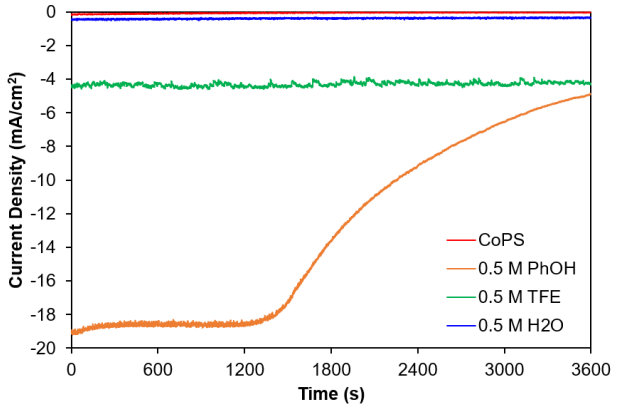

Figure S11. Controlled potential electrolysis traces measured under nitrogen atmosphere. In all cases a solution of 1 mM **CoPS** in acetonitrile (with 0.1 M [nBu$_4$N][PF$_6$] supporting electrolyte) was held at a potential of -2.18 V for 1 hour in the absence of acid (red), presence of 0.5 M PhOH (orange), presence of 0.5 M TFE (green), or presence of 0.5 M water (blue).

Table S11. Summary of CPE results under nitrogen atmosphere. All data presented are averaged quantities of multiple experiments, as reflected in the determined error bars. Charge passed was determined by integration of the CPE trace, and gaseous products were determined by gas chromatography.

	Potential (V)	Duration (h)	Charge (C)	mol H_2	mol CO	TON H_2
No acid	-2.18	1	2.72±0.2	-	-	-
PhOH	-2.18	1	94.66±4.7	5.34±0.5E-04	-	16.59
TFE	-2.18	1	38.62±1.9	2.08±0.2E-04	-	5.29
H_2O	-2.18	1	3.42±0.74	4.67±0.6E-05	-	1.19

Table S12. Summary of results from CPE experiments under nitrogen atmosphere. All data presented are averaged quantities of multiple experiments, as reflected in the determined error bars. Charge passed was determined by integration of the CPE trace, and gaseous products were determined by gas chromatography.

	Potential (V)	Duration (h)	FE (H_2)
No acid	-2.18	1	-
PhOH	-2.18	1	>99%
TFE	-2.18	1	>99%
H_2O	-2.18	1	26±2%

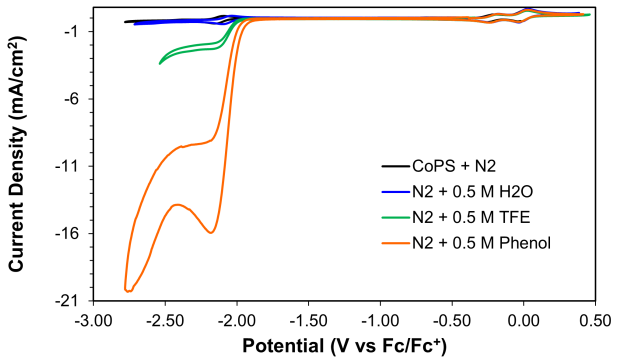

Figure S12. Cyclic voltammetry of 1 mM **CoPS** in acetonitrile with 0.1 M [nBu$_4$N][PF$_6$] supporting electrolyte at 100 mV/s under N_2 atmosphere with no acid (black) and with 0.5 M water (blue), 0.5 M TFE (green), and 0.5 M PhOH (orange).

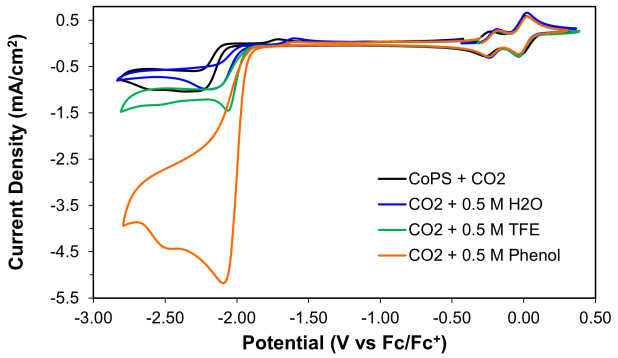

Figure S13. Cyclic voltammetry of 1 mM **CoPS** in acetonitrile with 0.1 M [nBu$_4$N][PF$_6$] supporting electrolyte at 100 mV/s under CO_2 atmosphere with no acid (black) and with 0.5 M water (blue), 0.5 M TFE (green), and 0.5 M PhOH (orange).

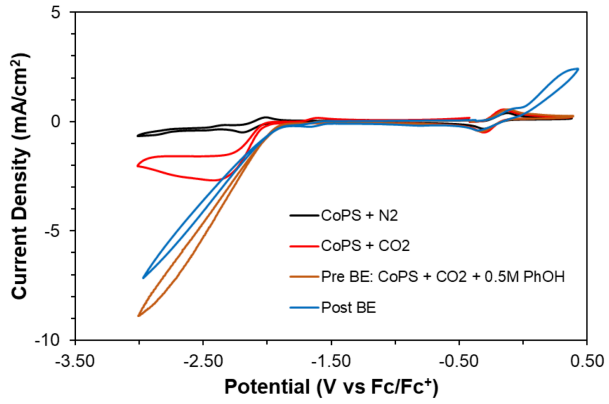

Figure S14. Cyclic voltammetry of 1 mM **CoPS** in acetonitrile with 0.1 M [nBu$_4$N][PF$_6$] supporting electrolyte at 100 mV/s under N_2 atmosphere (black), CO_2 atmosphere with no acid (red), as well as with 0.5 M PhOH before (brown) and after (blue) CPE studies.

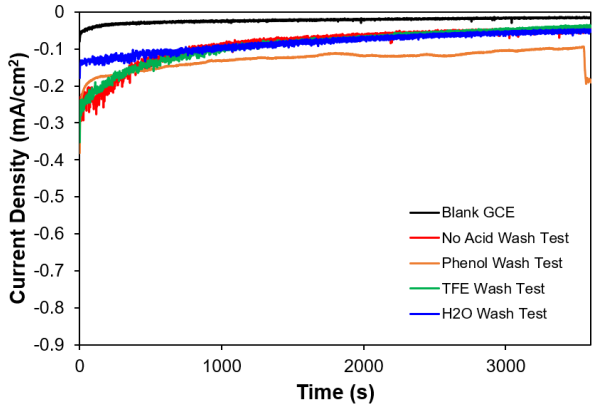

Figure S15. Rinse test traces measured under catalytic conditions. In all cases, the CPE solutions were removed from the electrolysis cell by syringe and the cell was rinsed with acetonitrile. A typical CPE blank trace in the absence of catalyst is shown for comparison (black). Slightly higher currents are generated than in the blank experiment, though no detectable products were generated.

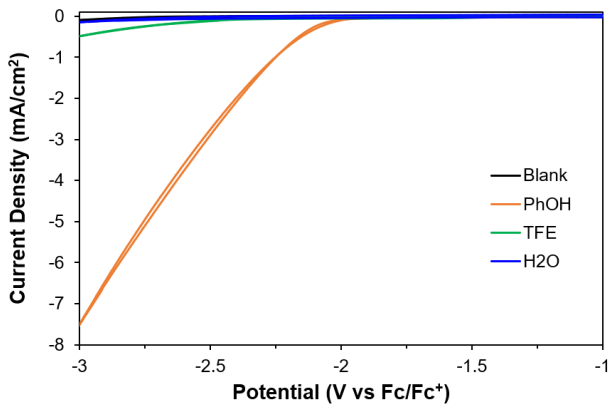

Figure S16. Cyclic voltammetry of a glassy carbon working electrode in acetonitrile with 0.1 M [nBu$_4$N][PF$_6$] supporting electrolyte (scan rate = 100 mV/s) under N_2 atmosphere in the presence of various acid additives at a concentration of 0.5 M.

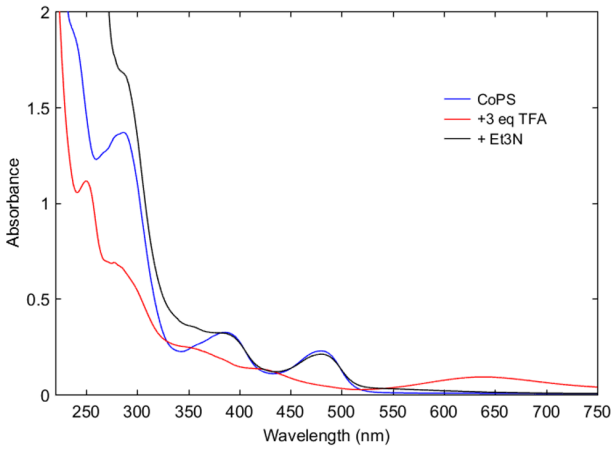

Figure S17. Overlay of the UV-Vis spectra of 1 mM **CoPS** in acetonitrile (blue) with the addition of 3 eq TFA (red) and subsequent addition of excess triethylamine (black).

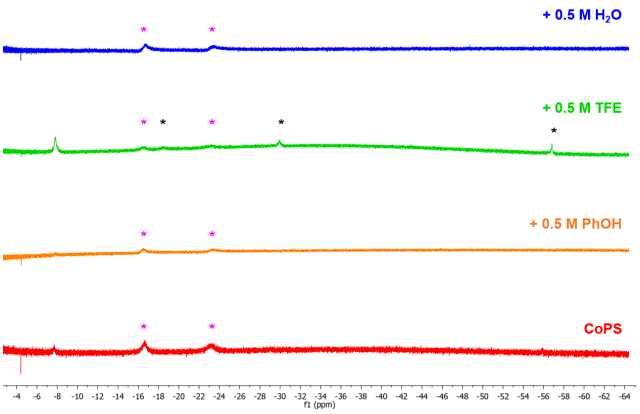

Figure S18. ^{1}H-NMR spectra of 1 mM **CoPS** in acetonitrile-d_3 without acid additive (red), with 0.5 M PhOH (orange), with 0.5 M TFE (green), and with 0.5 M H_2O (blue). Pink asterisks mark characteristic ^{1}H-NMR signatures of **CoPS**, and black asterisks mark the corresponding shifted features associated with protonation.

Table S13. Thermodynamic potential for CO_2 reduction to CO in the presence of various proton sources, and overpotential associated with **CoPS**.

Acid	pK_a[12]	E° (CO_2/CO) V vs Fc/Fc^+	η (V)
None	N/A	–0.12	2.06
H_2CO_3	23.4	–1.55	0.63
PhOH	29.1	–1.9	0.28
TFE	35.4	–2.12	0.06

Nuclear Coordinates for Optimized Geometries

Table S14. Nuclear coordinates for **[CoPS]^0**.

I	Atom	X	Y	Z
1	P	-0.0581365	1.4105284	-1.6631213
2	C	0.3164792	1.0575953	-4.51082
3	H	0.1488916	2.1321935	-4.6482454
4	C	0.5561038	0.2505782	-5.6317084
5	H	0.5856512	0.6945876	-6.6317293
6	C	0.7569329	-1.1289419	-5.460891

7	H	0.9479966	-1.764518	-6.3323773
8	C	0.7139462	-1.702368	-4.1847644
9	H	0.8682751	-2.7782047	-4.0528856
10	C	0.4740188	-0.8922299	-3.0571127
11	S	0.4105619	-1.6091933	-1.4245911
12	Co	0.1668392	0.0006665	0.0056878
13	C	0.4578328	0.8980962	3.0690565
14	C	0.6861136	1.7112492	4.1969762
15	H	0.8309909	2.7883674	4.0648538
16	C	0.7297138	1.139135	5.4736519
17	H	0.9115288	1.7770507	6.3454083
18	C	0.5413317	-0.2421275	5.6446789
19	H	0.5715759	-0.6851637	6.6451097
20	C	0.3133115	-1.052128	4.5235305
21	H	0.1554057	-2.1281712	4.6611363
22	C	0.275197	-0.4896463	3.2354209
23	P	-0.050695	-1.4101178	1.6749594
24	C	-1.8200298	2.0573828	-1.9161794
25	H	-1.7236667	2.8721307	-2.662839
26	C	1.0614954	2.9121686	-1.8884827
27	H	0.943786	3.1785149	-2.9572683
28	C	-1.807954	-2.0706887	1.9249585
29	H	-1.7067185	-2.8831896	2.6734241
30	C	1.0803098	-2.9023643	1.9046763
31	H	0.9601303	-3.1697412	2.9729383
32	C	0.2794222	0.4939567	-3.2232109
33	C	-2.7230346	0.9558366	-2.4951662
34	H	-2.7752016	0.089405	-1.811348
35	H	-3.7491932	1.3468055	-2.6203866
36	H	-2.3699592	0.5933666	-3.4731029
37	C	-2.4273356	2.6199642	-0.6209783
38	H	-3.3775961	3.1352962	-0.8515217
39	H	-2.6481923	1.8034141	0.0874017
40	H	-1.7647788	3.3272921	-0.0994658
41	C	0.6882698	4.141969	-1.0502235
42	H	-0.3137952	4.5287332	-1.2999033
43	H	0.721977	3.9250455	0.029654
44	H	1.4129737	4.9517715	-1.2534997
45	C	2.5172071	2.4760621	-1.6567297
46	H	2.7814054	1.6009621	-2.2745061
47	H	3.2051222	3.30047	-1.9188195
48	H	2.6842685	2.2122912	-0.5987827
49	S	0.3949092	1.6131884	1.43573
50	C	-2.7218953	-0.9759475	2.4995603
51	H	-3.7443797	-1.3764285	2.624753

52	H	-2.3732036	-0.6073236	3.4767555
53	H	-2.7816791	-0.1122938	1.8128882
54	C	-2.4069806	-2.6400459	0.6289247
55	H	-3.3546051	-3.1613453	0.8569565
56	H	-2.6306058	-1.8258579	-0.081225
57	H	-1.7379408	-3.3438015	0.1108923
58	C	0.7213341	-4.1354495	1.0648952
59	H	-0.2792311	-4.5294599	1.3090511
60	H	0.7595295	-3.919387	-0.015028
61	H	1.4508609	-4.9396757	1.2730424
62	C	2.533256	-2.4537759	1.6792806
63	H	2.7028323	-2.1882454	0.6221722
64	H	2.7875224	-1.5766464	2.298269
65	H	3.2271377	-3.272259	1.9441539

Nuclear Repulsion Energy = 4607.7682230237 hartrees

Table S15. Nuclear coordinates for **[CoPS]**$^{-}$.

I	Atom	X	Y	Z
1	P	-0.0303905	1.3400189	-1.5814805
2	C	-0.1645212	0.9598697	-4.4655509
3	H	-0.5402877	1.9879027	-4.5610368
4	C	0.0294181	0.1900945	-5.6237588
5	H	-0.1896305	0.6102096	-6.6120458
6	C	0.5129415	-1.1269951	-5.4962236
7	H	0.6737158	-1.7386491	-6.392968
8	C	0.7848638	-1.666397	-4.2355824
9	H	1.1528393	-2.6945905	-4.1394429
10	C	0.5830394	-0.8982409	-3.0638602
11	S	0.9062815	-1.5531273	-1.4502872
12	Co	0.4578341	0.0047601	0.0082007
13	C	0.562781	0.9054808	3.0812964
14	C	0.7516125	1.6745328	4.2546081
15	H	1.1067907	2.7074308	4.1607993
16	C	0.4829271	1.1300373	5.5137663
17	H	0.6334549	1.7423551	6.4118242
18	C	0.0154177	-0.1931502	5.6381106
19	H	-0.2013037	-0.6173133	6.6251925
20	C	-0.1657096	-0.9636375	4.4783433
21	H	-0.5296821	-1.9961383	4.5712305
22	C	0.1059728	-0.4329604	3.2058953
23	P	-0.021661	-1.3376976	1.5941802
24	C	-1.7635874	2.1136798	-1.6617508
25	H	-1.7178458	2.9093025	-2.4349219

26	C	1.0949442	2.8186687	-2.0241815
27	H	0.8540248	3.0820205	-3.0737729
28	C	-1.7492807	-2.1243012	1.6676635
29	H	-1.7010491	-2.9197587	2.4408242
30	C	1.1131128	-2.8086332	2.0390427
31	H	0.8703307	-3.0746421	3.0875503
32	C	0.1097811	0.4342196	-3.1915557
33	C	-2.8033319	1.0638844	-2.0759351
34	H	-2.7774024	0.2178774	-1.3655151
35	H	-3.8214086	1.4989255	-2.053709
36	H	-2.6142851	0.6625757	-3.0843342
37	C	-2.1597143	2.7373122	-0.3141419
38	H	-3.0987152	3.3147595	-0.4234264
39	H	-2.3254427	1.9463093	0.4374988
40	H	-1.3832489	3.397404	0.099758
41	C	0.9231116	4.0714656	-1.1540201
42	H	-0.0683704	4.5387566	-1.2852184
43	H	1.0539765	3.8366091	-0.0837984
44	H	1.6845867	4.8276299	-1.4302082
45	C	2.5415948	2.3029704	-1.9710178
46	H	2.6615319	1.3811678	-2.5659602
47	H	3.2456763	3.066252	-2.3563329
48	H	2.821327	2.0618592	-0.9305302
49	S	0.8812719	1.5668876	1.4693731
50	C	-2.79716	-1.0810999	2.0779973
51	H	-3.8130133	-1.5208125	2.0477449
52	H	-2.6167564	-0.6819311	3.0888317
53	H	-2.7701961	-0.2326573	1.3705631
54	C	-2.1350555	-2.7503104	0.318281
55	H	-3.0734319	-3.3297879	0.4219308
56	H	-2.2967202	-1.9609566	-0.4360222
57	H	-1.3540718	-3.40935	-0.0886414
58	C	0.9541844	-4.0624663	1.1677574
59	H	-0.0333046	-4.5389181	1.2963318
60	H	1.085429	-3.8257974	0.0980191
61	H	1.7218708	-4.8118001	1.4453865
62	C	2.5561473	-2.2823219	1.9920765
63	H	2.8398793	-2.0416799	0.9525773
64	H	2.6658078	-1.3582615	2.5855578
65	H	3.2637382	-3.0395081	2.3829528

Nuclear Repulsion Energy = 4624.6743801470 hartrees

Table S16. Nuclear coordinates for **[CoPS]**$^{2-}$.

I	Atom	X	Y	Z
1	P	-0.1510368	1.0827326	-1.6374724
2	C	0.7097716	1.0307457	-4.4347808
3	H	0.0024507	1.853167	-4.6188167
4	C	1.4774011	0.5449273	-5.5085652
5	H	1.3805732	0.9855728	-6.5101617
6	C	2.3731231	-0.5169702	-5.272525
7	H	2.9836516	-0.9161469	-6.0957335
8	C	2.489105	-1.0694629	-3.9924044
9	H	3.1808803	-1.9025024	-3.8117051
10	C	1.7340217	-0.5754894	-2.8961252
11	S	1.8916188	-1.2747525	-1.2832844
12	Co	0.6018986	0.0761318	0.053662
13	C	1.5975346	0.6357106	3.05739
14	C	2.3269816	1.087734	4.1882019
15	H	2.9590203	1.9781185	4.0752793
16	C	2.2635076	0.4200607	5.4166593
17	H	2.8578759	0.7857909	6.2668463
18	C	1.4439489	-0.7161922	5.5662044
19	H	1.3911587	-1.2468975	6.5266263
20	C	0.6958705	-1.1588959	4.460079
21	H	0.0402136	-2.0348349	4.5771054
22	C	0.7661979	-0.5194179	3.208761
23	P	-0.1820586	-1.0263911	1.6701495
24	C	-1.8991134	0.7985361	-2.4377207
25	H	-1.9038804	1.3091414	-3.4233782
26	C	-0.0502536	2.996869	-1.8665999
27	H	-0.6262808	3.3004314	-2.7689535
28	C	-1.9327528	-0.7668133	2.4696726
29	H	-1.9335877	-1.3008318	3.4430215
30	C	-0.0977747	-2.9501205	1.770802
31	H	-0.6893912	-3.3089374	2.6423417
32	C	0.8245116	0.5037155	-3.1348288
33	C	-2.077279	-0.7075706	-2.6586583
34	H	-2.0306547	-1.243003	-1.6915407
35	H	-3.054377	-0.9297889	-3.1381442
36	H	-1.2711897	-1.1169424	-3.2913269
37	C	-3.038412	1.3504084	-1.5753717
38	H	-4.0244791	0.9552251	-1.9002795
39	H	-2.8827591	1.0524761	-0.5198003
40	H	-3.0956868	2.4524222	-1.6112242
41	C	-0.633706	3.6988084	-0.6297715
42	H	-1.6808653	3.4131309	-0.4370245

43	H	-0.0526912	3.4207748	0.2679801
44	H	-0.5932866	4.803136	-0.7453795
45	C	1.41677	3.418048	-2.0390802
46	H	1.8498429	3.0375749	-2.9791896
47	H	1.5158508	4.5240469	-2.0279995
48	H	2.0196292	3.0123014	-1.2056026
49	S	1.6931667	1.4729835	1.5045094
50	C	-2.1047788	0.7348482	2.7264186
51	H	-3.0932238	0.9527076	3.1841923
52	H	-1.313986	1.1180037	3.3936172
53	H	-2.0221226	1.2971399	1.7764939
54	C	-3.0725114	-1.2987131	1.5964442
55	H	-4.057768	-0.9075105	1.9283795
56	H	-2.9165192	-0.9814195	0.5470248
57	H	-3.1319462	-2.4012492	1.6111595
58	C	-0.6739075	-3.5421035	0.4738312
59	H	-1.7446752	-3.3140958	0.3421931
60	H	-0.1362974	-3.1143131	-0.3926534
61	H	-0.5539328	-4.6463978	0.4555153
62	C	1.3613193	-3.4052465	1.9268566
63	H	1.9709702	-2.997626	1.1002886
64	H	1.8062369	-3.0589678	2.8745649
65	H	1.4338027	-4.5128964	1.8888107

Nuclear Repulsion Energy = 4577.4152397201 hartrees

References:

1. Barry, B. M.; Stein, B. W.; Larsen, C. A.; Wirtz, M. N.; Geiger, W. E.; Waterman, R.; Kemp, R. A. Metal Complexes (M = Zn, Sn, and Pb) of 2-Phosphinobenzenethiolates: Insights into Ligand Folding and Hemilability. *Inorg. Chem.* **2013**, 52, 9875–9884.
2. (a) Sheldrick, G. M. Phase Annealing in SHELX-90: Direct Methods for Larger Structures. *Acta Cryst.* **1990**, A46, 467. (b) Sheldrick, G. M. A Short History of SHELX. *Acta Cryst.* **2008**, A64, 112. (c) Müller, P. Practical Suggestions for Better Crystals. *Cryst. Rev.* **2009**, 15, 57.
3. (a) Cotton, F. A.; Wilkinson, G. *Advanced Inorganic Chemistry*, 4th ed.; Wiley: New York, 1980. (b) Chapovetsky, A.; Welborn, M.; Luna, J. M.; Haiges, R.; Miller, T. F.; Marinescu, S. C. Pendant Hydrogen-Bond Donors in Cobalt Catalysts Independently Enhance CO_2 Reduction. *ACS Cent. Sci.* **2018**, 4, 397–404.

4. (a) Costentin, C.; Drouet, S.; Robert, M.; Savéant, J. M. A Local Proton Source Enhances CO_2 Electroreduction to CO by a Molecular Fe Catalyst. *Science* **2012**, 338, 90−94. (b) Costentin, C.; Savéant, J.-M. Multielectron, Multistep Molecular Catalysis of Electrochemical Reactions: Benchmarking of Homogeneous Catalysts. *ChemElectroChem* **2014**, 1, 1226–1236.
5. Shao, Y.; Molnar, L.; Jung, Y.; Kussmann, J.; Ochsenfeld, C.; Brown, S.; Gilbert, A.; Slipchenko, L.; Levchenko, S.; O'Neill, D.; DiStasio, R.; Lochan, R.; Wang, T.; Beran, G.; Besley, N.; Herbert, J.; Lin, C.; Van Voorhis, T.; Chien, S.; Sodt, A.; Steele, R.; Rassolov, V.; Maslen, P.; Korambath, P.; Adamson, R.; Austin, B.; Baker, J.; Byrd, E.; Dachsel, H.; Doerksen, R.; Dreuw, A.; Dunietz, B.; Dutoi, A.; Furlani, T.; Gwaltney, S.; Heyden, A.; Hirata, S.; Hsu, C.; Kedziora, G.; Khalliulin, R.; Klunzinger, P.; Lee, A.; Lee, M.; Liang, W.; Lotan, I.; Nair, N.; Peters, B.; Proynov, E.; Pieniazek, P.; Rhee, Y.; Ritchie, J.; Rosta, E.; Sherrill, C.; Simmonett, A.; Subotnik, J.; Woodcock, H.; Zhang, W.; Bell, A.; Chakraborty, A.; Chipman, D.; Keil, F.; Warshel, A.; Hehre, W.; Schaefer, H.; Kong, J.; Krylov, A.; Gill, P.; Head-Gordon, M. Advances in Methods and Algorithms in a Modern Quantum Chemistry Program Package. *Phys. Chem. Chem. Phys.* **2006**, 8, 3172-3191.
6. Perdew, J. P.; Burke, K.; Ernzerhof, M. Generalized Gradient Approximation Made Simple. *Phys. Rev. Lett.* **1996**, 77, 3865–3868.
7. Ditchfield, R.; Hehre, W. J.; Pople, J. A. Self-Consistent Molecular-Orbital Methods. IX. An Extended Gaussian-Type Basis for Molecular-Orbital Studies of Organic Molecules. *J. Chem. Phys.* **1971**, 54, 724–728.
8. Hehre, W. J.; Ditchfield, K.; Pople, J. A. Self-Consistent Molecular Orbital Methods. XII. Further Extensions of Gaussian-Type Basis Sets for Use in Molecular Orbital Studies of Organic Molecules. *J. Chem. Phys.* **1972**, 56, 2257–2261.
9. Weigend, F.; Ahlrichs, R. Balanced basis sets of split valence, triple zeta valence and quadruple zeta valence quality for H to Rn: Design and assessment of accuracy *Phys. Chem. Chem. Phys.* **2005**, 7, 3297.
10. Feller, D. The role of databases in support of computational chemistry calculations *J. Comput. Chem.* **1996**, 17, 1571-1586.

11. Schuchardt, K. L.; Didier, B. T.; Elsethagen, T; Sun, L.; Gurumoorthi, V.; Chase, J.; Li, J.; Windus, T. L. Basis Set Exchange: A Community Database for Computational Sciences *J. Chem. Inf. Model.* **2007**, 47, 1045-1052.

12. (a) Clark, M. L.; Cheung, P. L.; Lessio, M.; Carter, E. A.; Kubiak, C. P. Kinetic and Mechanistic Effects of Bipyridine (Bpy) Substituent, Labile Ligand, and Brønsted Acid on Electrocatalytic CO_2 Reduction by Re(Bpy) Complexes. *ACS Catal.* **2018**, 8, 2021–2029. (b) Matsubara, Y.; Grills, D. C.; Kuwahara, Y. *ACS Catal.* **2015**, 5, 6440-6452.

13. Machan, C. W.; Sampson, M. D.; Kubiak, C. P. A Molecular Ruthenium Electrocatalyst for the Reduction of Carbon Dioxide to CO and Formate. *J. Am. Chem. Soc.* **2015**, 137, 8564−8571.

14. Yang, L.; Powell, D. R.; Houser, R. P. Structural variation in copper(I) complexes with pyridylmethylamide ligands: structural analysis with a new four-coordinate geometry index, τ_4. *J. Chem. Soc. Dalt. Trans.* **2007**, 955–964.